An innovative seismic SSI zonation for the city of Catania (Italy)

Glenda Abate[a], Simone Bramante[a], Sebastiano Corsico[a], Salvatore Grasso[a], Maria Rossella Massimino[a]
[a] *Department of Civil Engineering and Architecture, Via Andrea Doria 6, 95125, Catania, Italy*

Keywords: Soil Structure Interaction, Site response, Fundamental period, Spectral acceleration, Urban mapping

ABSTRACT
The present paper shows a methodology for a large-scale estimate of soil-structure interaction (SSI) effects in the urban area of Catania (Italy), that is characterized by a high seismic risk. The proposed procedure combines geotechnical characteristics of the soil achieved by field surveys with buildings features (height and foundation geometry) and construction type of the buildings (masonry or concrete) known by means of in-situ inspection. Moreover, the seismic hazard and the site effects are evaluated for the analysed areas using 2 artificial inputs and 3 inputs recorded recently in Catania, including the very recent earthquake which hit Catania in 26th December 2018. Preliminary, 1-D seismic response analyses are performed. The building fundamental periods, the response spectra and the related spectral accelerations are evaluated for more than 200 buildings, considering both the fixed-base building configuration and the flexible-base one.
The achieved results allow us to obtain important consideration on SSI effects in order to develop an innovative seismic microzonation map of Catania. The results are also compared with the prescriptions of the Italian Technical Code (NTC2018). Spatially distributed ratios of the structural fundamental periods and the related spectral accelerations corresponding to flexible-base over fixed-base conditions are mapped in Google My Maps environment.

1 INTRODUCTION

The observation of the damage caused by recent earthquakes has shown that a seismic structural design is not always sufficient to have good safety conditions if soil behavior is not appropriately taken into account. So, foundation soil seismic behaviour and, above all, dynamic soil-structure interaction (DSSI), have an important role to determine the dynamic behavior of the structure: recent seismic microzonation studies are moving in this direction. Despite the effects of DSSI, the structural design is commonly based on the assumption of fixed-base structures.

A flexible-base structure has an higher fundamental period compared to this one of a fixed-base structure (Figure 1); so the spectral ordinates corresponding to the fixed-base structure are higher than flexible-base case. But sometimes the trend of the response spectra is such to modify this behavior, and this leads to an underestimation of the seismic actions.

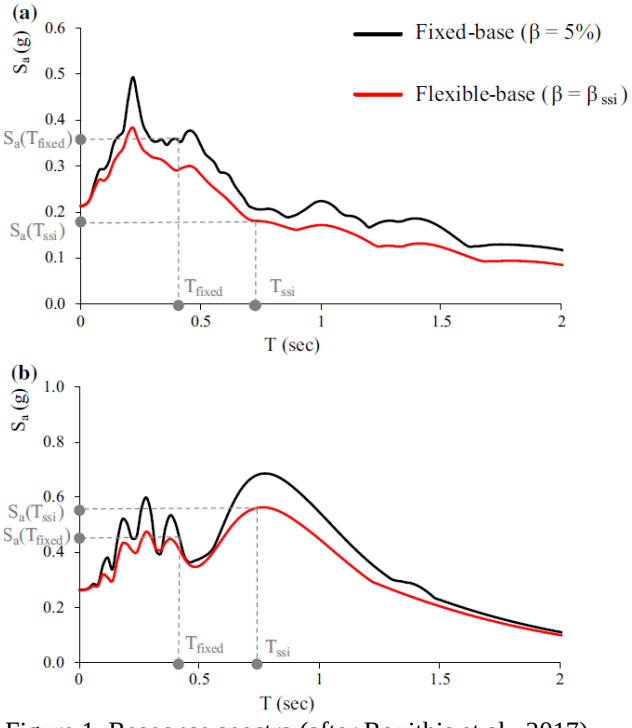

Figure 1. Response spectra (after Rovithis et al., 2017).

According to this affirmation, a procedure for a large-scale estimate of DSSI effects is proposed.

This methodology combines the characteristics of the structure (height, foundation geometry, materials) with the geotechnical characteristics of the foundation soil. The study refers to several seismic inputs characteristic for the Catania area at the bedrock level. These inputs are used for 1-D seismic response analyses, which support subsequent analyses of DSSI effects. Microzonation maps in terms of T_{ssi}/T_{fixed}, $S_a(T_{ssi})/S_a(T_{fixed})$ and $S_a(T_{ssi})/S_a(NTC18)$ ratios for a representative initial area involving more than 200 buildings are developed, being: T_{ssi} and T_{fixed} the fundamental period of the flexible-base and the fixed-base structure, respectively; $S_a(T_{ssi})$ and $S_a(T_{fixed})$ the corresponding spectral accelerations evaluated considering or ignoring DSSI and $S_a(NTC18)$ the spectral acceleration evaluated according to NTC_2018.

The achieved results allow us to develop an innovative seismic microzonation map of Catania, useful for planning the retrofitting of the investigated buildings, most of which were built before the modern seismic codes. Finally, interesting consideration are developed on the reliability of NTC_2018 prescriptions.

2 EVALUATION OF DSSI EFFECTS

A soil-structure system may be modelled by an equivalent oscillator with allowable translational and rocking motion of its base (Veletsos and Meek, 1974). Its effective period (T_{ssi}) may be computed by means of the following formula adopted in BSSC (2009):

$$T_{ssi} = T_{fixed}\sqrt{1 + \frac{k_{str}}{k_h} + \frac{k_{str}{h_{eff}}^2}{k_r}} \quad (1)$$

where T_{fixed} and k_{str} refer to the fundamental period and the horizontal stiffness of the fixed-base structure, h_{eff} is the effective height of the structure equal to $0.7H$ (except for single-storey buildings where $h = H$), while k_h and k_r are the translational and rocking stiffness of the foundation, respectively (Rovithis et al., 2017). The above formula refers to a single isolated structure, but in this study it is extended to an urban context where adjacent structures are present. Obviously, multiple interactions between structures of a building cluster may further affect the resulting seismic response due to combined soil-structure (SSI) and structure-soil-structure (SSSI) interaction phenomena (Gueguen et al., 2002; Knappett et al., 2015). However, about the fundamental periods of the system, the additional effects of SSSI are negligible if compared to the effect of just the SSI and thus they are not taken into account (Isbiliroglu et al., 2015).

The fundamental period of the fixed-base structure (T_{fixed}) is estimated according to the formula suggested by the old Italian Technical Code (NTC_2008):

$$T_{fixed} = C_1 H^{3/4} \quad (2)$$

where C_1 is equal to 0.075 for concrete structures and 0.050 for masonry structures, while H is the height of the structure.

The horizontal stiffness of the fixed-base structure k_{str} is obtained by reversing the known formula:

$$k_{str} = \frac{4\pi^2}{T_{fixed}^2} m \quad (3)$$

where m is the mass of the structure.

The translational (k_h) and rocking (k_r) stiffness of the foundation may be computed by means of the following expressions (BSSC 2009):

$$k_h = \frac{8}{(2-\nu)} G r_a \quad (4)$$

$$k_r = \frac{8}{3(1-\nu)} G r_m^3 \alpha_\theta \quad (5)$$

where ν is the Poisson ratio of the soil, G is the shear modulus of soil and α_θ is a dimensionless coefficient that depends on the period of the excitation, the dimension of the foundation, and the properties of the supporting medium (Veletsos and Verbic, 1973) that is assumed equal to 1 without accurate studies.

In the above expressions, the foundation stiffness is taken into account by an equivalent rectangular surface foundation, according the procedure suggested by Gueguen et al. (2002) and Rovithis et al. (2017). According to FEMA 440 (2005), the equivalent radii of the whole foundation area of the structure in translational and rocking motion are:

$$r_a = \sqrt{A_0/\pi} \quad (6)$$

$$r_m = \sqrt[4]{4I_0/\pi} \quad (7)$$

where A_0 and I_0 stand for the area and the moment of inertia of the foundation, respectively. In particular, A_0 is the footprint area of each structure (it refers to a rectangular footprint area of dimension $B_{eq} = \sqrt{A_0}$); in this manner, the

moment of inertia of the foundation I_0 may be computed by $B_{eq}^4/12$.

The shear modulus of soil is introduced for each structure along an effective depth of soil equal to $0.75r_a$ and $0.75r_m$ for the translational and rocking stiffness of the foundation (Rovithis et al., 2017). In particular, the degradation of the shear modulus of soil is taken into account with the deformation level γ. So, the degradation coefficient is estimated according to the procedure suggested by the EC8 (section 5).

According to BSSC (2009), the effective damping factor β_{ssi} of a soil-structure system is defined as:

$$\beta_{ssi} = \beta_0 + \frac{\beta_{fixed}}{\left(\frac{T_{ssi}}{T_{fixed}}\right)^3} \quad (8)$$

where β_0 is a foundation damping factor depending on T_{ssi}/T_{fixed}. It is defined as:

$$\beta_0 = a_1\left(\frac{T_{ssi}}{T_{fixed}} - 1\right) + a_2\left(\frac{T_{ssi}}{T_{fixed}} - 1\right)^2 \quad (9)$$

where:

$$a_1 = c_e exp\left(4{,}7 - 1{,}6\frac{h_{eff}}{r_m}\right) \quad (10)$$

$$a_2 = c_e\left[25ln\left(\frac{h_{eff}}{r_m}\right) - 16\right] \quad (11)$$

$$c_e = 1{,}5\frac{e}{r_a} + 1 \quad (12)$$

In the above expressions, "e" is a coefficient taking into account the foundation depth that is assumed equal to 1 m without accurate studies.

The damping factor β_{ssi} is generally higher than the damping factor β_{fixed} related to the fixed-base structure. The latter is approximately equal to 5% for concrete structures and 8% for masonry structures, with the exception of the rare case of the foundation damping itself being very low (smaller than 5%), and the period ratio being large (Worku, 2014). In fact, the system damping gradually decreases with increasing period ratio. However, it should be noted that the effective damping may not generally be taken less than the structural damping of 5% (BSSC 2004, BSSC 2010).

These damping ratios will be used to plot the response spectra in accordance with the procedure proposed by Chopra (1995). Then, according to the periods T_{ssi} and T_{fixed} the spectral accelerations will be calculated and compared.

3 THE CATANIA CASE-HISTORY

The involved subsoil was systematically investigated by in-situ and laboratory geotechnical tests since 1998 within two important research projects involving the city of Catania (Faccioli, 2000; Maugeri, 2005), reaching a database of more than 1200 in-situ tests and allowing us to develop important site response analyses (Grasso et al., 2005a, b; Abate et al., 2006; Massimino et al., 2019).

Main litotypes are shown in Figure 2. The performed geotechnical tests (C-H, D-H and SASW) allowed us to find the shear wave velocity, whose spatial distribution is shown in Figure 3; instead, the corresponding values for each litotype are shown in Table 1. The surveys executed are identified in the Google My Maps environment (Figure 4).

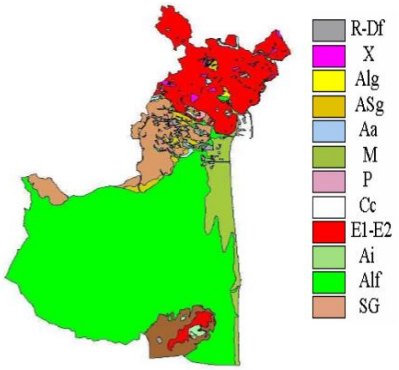

R-Df*: Top soil and fill (R); debris and landslides (Dt)*
X: *Scoriaceous lavas and volcanoclastic rocks*
Alg: *Coarse alluvial deposits (sands, gravels and pebbles)*
Asg: *Yellowish or brown clays ans sandy silts*
Aa: *Silty clays and grey-bluish marly clays*
M: *Marine deposits*
P: *Pyroclastic rocks*
Cc: *Calcarenites and block-calcarenites*
E1-E2: *Fractured to slightly fractured lavas*
Ai: *Clayey interlayers in Cc unit*
Alf: *Fine alluvial deposits*
SG: *Yellow or brown quartzose sands and sandstone, gravels and conglomerates with pyroclastic alternations*

Figure 2. Geotechnical map of the city of Catania (after Faccioli et al., 2000).

In particular, different layers are loaded, in order to identify the survey, the height of the buildings, the type of structure. The layer shown in Figure 4 sreports the different surveys, marked by a specific tag. In particular, the surveys near the buildings are taken into account for identifying the soil stratigraphy. So, the geotechnical parameters corresponding to the different structures are identified.

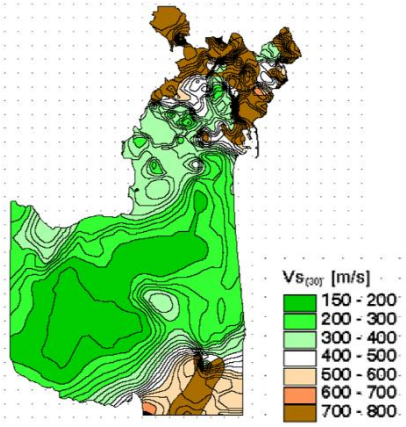

Figure 3. Spatial distribution of shear-wave velocity for the city of Catania (after Faccioli et al., 2000).

Table 1. Characteristic values of some representative geotechnical parameters (see Figure 2).

litotype	γ [kN/m^3]	V_S [m/s]
R-Df	17.0 ÷ 19.0	130 ÷ 220
X	18.0 ÷ 18.5	180 ÷ 300
Alg	18.0 ÷ 19.5	210 ÷ 280
Asg	19.3 ÷ 20.0	220 ÷ 400
Aa	19.5 ÷ 20.0	450 ÷ 600
M	18.3 ÷ 18.7	210 ÷ 280
P	16.0 ÷ 17.0	250 ÷ 500
Cc	21.0 ÷ 23.5	500 ÷ 800
E1-E2	22.0 ÷ 24.0	350 ÷ 500
Ai	21.0 ÷ 23.5	300 ÷ 650
Alf	18.5 ÷ 19.5	130 ÷ 210
SG	19.8 ÷ 20.8	350 ÷ 500

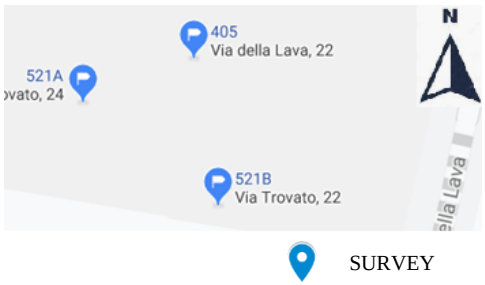

Figure 4. The surveys identified in the Google My Maps environment.

3.1 *The investigated area and the utilised inputs*

The investigated area is located in the North-East area of the city of Catania. It covers 17,2 hectares and includes 212 buildings; they include both masonry (111) and concrete structures (101).

According to the stratigraphy of foundation soil, the area is divided into 3 areas: T1, T2 and T3 (Figure 5). The first one is characterized by the presence of top soil and fill (low shear-wave velocity) the second and the third ones are characterized by rocks soils (high shear-wave velocity). Figure 6 shows the V_s profiles for the three stratigraphies, as well as the litotypes present in each stratigraphy.

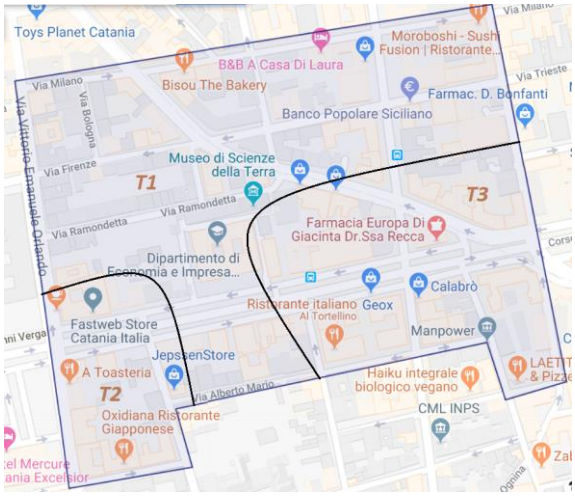

Figure 5. The investigated area and the three considered sub-areas.

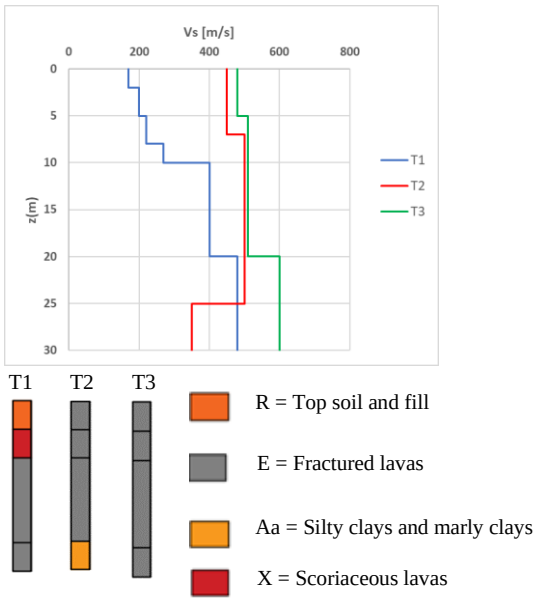

Figure 6. Profiles of V_s for the three considered sub-areas and the corresponding stratigraphies.

Finally, five seismic inputs have been applied to the conventional bedrock. They represent the scenario earthquakes expected for the given area and for a specified period of return. So, the seismic hazard is evaluated for the analysed areas using 2 artificial inputs and 3 inputs recorded recently in Catania.
In particular, one synthetic accelerogram evaluated assuming the source to be along the Hyblean-Maltese fault and generating the 1693 seismic ground motion scenario (Grasso et al., 2005; Laurenzano et al., 2004); one synthetic accelerograms evaluated assuming the source to be along the Hyblean-Maltese fault and generating the 1818 seismic ground motion

scenario (Grasso et al., 2005); three inputs recorded during the 1990, 2002 and 2018 earthquakes at the Sortino, Catania and Santa Venerina station, respectively.

In order to fit the accelerograms at the reference area, they have been scaled at the same maximum expected acceleration (PGA = 0.206 g), corresponding to the SLV state (i.e. the limit state for the safety of human life) and considering the buildings of class II (corresponding to the return period of 475 years), according to NTC_2018. Table 2 shows the main characteristics of the inputs used; while Figure 7 shows their time histories.

Table 2. Main characteristics of inputs.

Date	Richter scale	f [Hz]	Epicenter
09.01.1693	M=7.4	0.42	Val di Noto
20.02.1818	M=6.0	0.58	Aci S. Antonio
13.12.1990	M=5.7	1.59	Augusta
29.10.2002	M=4.4	0.35	S. Venerina
26.12.2018	M=4.8	2.55	Etna

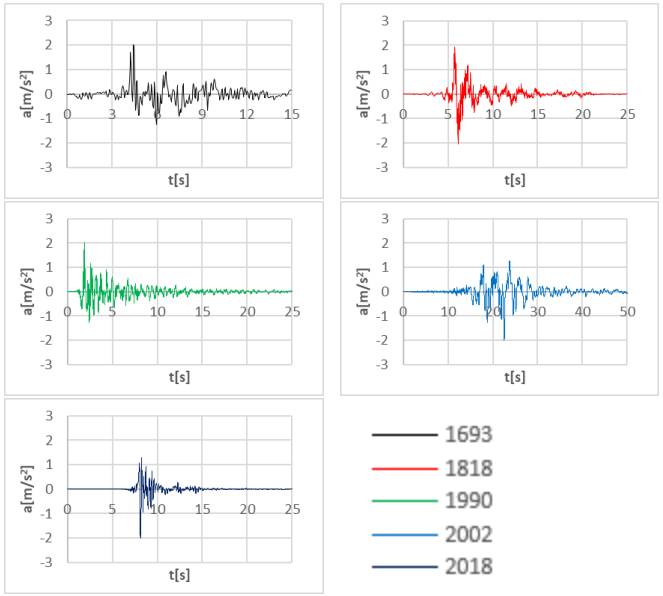

Figure 7. Utilised inputs scaled to the maximum expected acceleration (PGA = 0.206 g).

4 THE 1-D SITE RESPONSE ANALYSIS

Preliminarily, 1-D seismic response analyses are performed by means of Strata code (Kottke et al., 2013), adopting all the 5 inputs.

For lack of space, Figure 8 reports only the results of the seismic response analysis for the 1818 seismic input for the three considered sub-areas. The T1 stratigraphy amplifies the signal more than the others stratigraphies, due to its poor dynamic characteristics; on the contrary, T2 and T3 stratigraphies present mainly rock soils and so a negligible amplification occurs. For the same reasons, just the Fourier spectrum concerning the T1 stratigraphy present higher peaks compared to the other ones.

The results of this preliminary 1-D seismic response analysis are used for evaluating DSSI effects as reported in the next paragraph.

5 NEW SEISMIC MICROZONATION MAPS ACCORDING TO DSSI FOR THE INVESTIGATED AREA

The investigated area is further divided into 15 blocks, according to the urban morphology (Figure 9). Table 3 shows the number of structures present in each block.

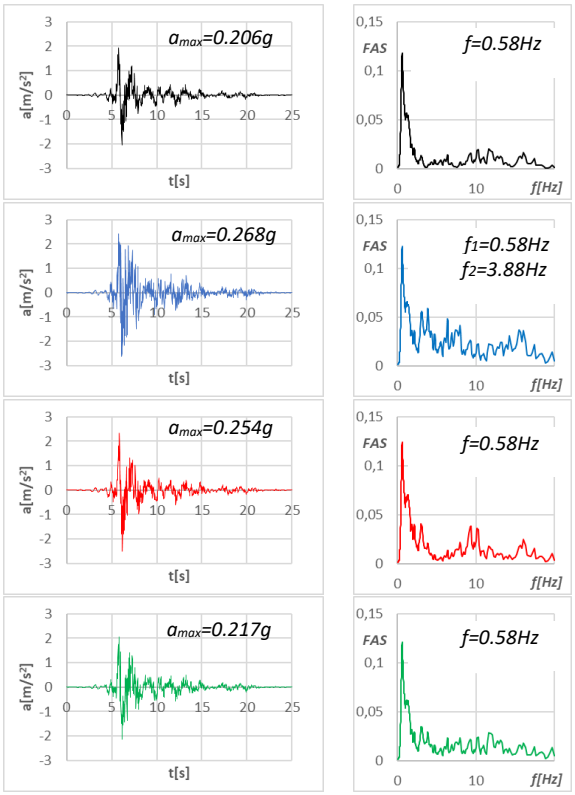

Figure 8. Results of 1-D response analysis for the 1818 seismic input: a) bedrock; b) "T1" stratigraphy; c) "T2" stratigraphy; d) "T3" stratigraphy.

In accordance with the procedure reported in BSSC (2009), for all the structures both the fixed-base building configuration and the flexible-base one are taken into account in order to evaluate the building fundamental periods, the response spectra and the related spectral accelerations. The results allow us to achieve important consideration on DSSI effects in order to develop an innovative seismic microzonation map.

These results are mapped in Google My Maps environment and shown in the following Figures 10-20.

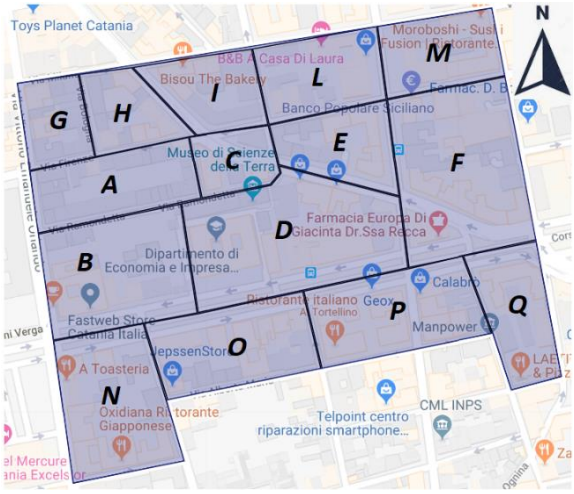

Figure 9. Division of the area.

Table 3. Number of structures in each block.

Block	Structures
A	34
B	19
C	8
D	15
E	12
F	22
G	13
H	14
I	8
L	12
M	6
N	11
O	17
P	13
Q	8

The T_{ssi}/T_{fixed} ratios are shown in Figure 10. Three different ranges are selected for indicate negligible (T_{ssi}/T_{fixed} < 1.15), moderate (1.15 < T_{ssi}/T_{fixed} < 1.30) and high (T_{ssi}/T_{fixed} ≥ 1.30) SSI effects on the fundamental period of the structures.

Negligible DSSI effects, (T_{ssi}/T_{fixed} < 1.15), are observed mainly for the "T2" and "T3" stratigraphies, characterized mainly by rock soils. So, for these cases, the assumption of fixed-base structure is acceptable.

The $S_a(T_{ssi})/S_a(T_{fixed})$ spectral acceleration ratios are shown in Figures 11-15, referred to the 5 adopted seismic inputs. As previously seen for the T_{ssi}/T_{fixed} ratios, three different ranges are selected for indicate beneficial ($S_a(T_{ssi})/S_a(T_{fixed})$ ≤ 0.85), negligible (0.85 < $S_a(T_{ssi})/S_a(T_{fixed})$ ≤ 1.15) and detrimental ($S_a(T_{ssi})/S_a(T_{fixed})$ > 1.15) DSSI effects on the seismic response of structures.

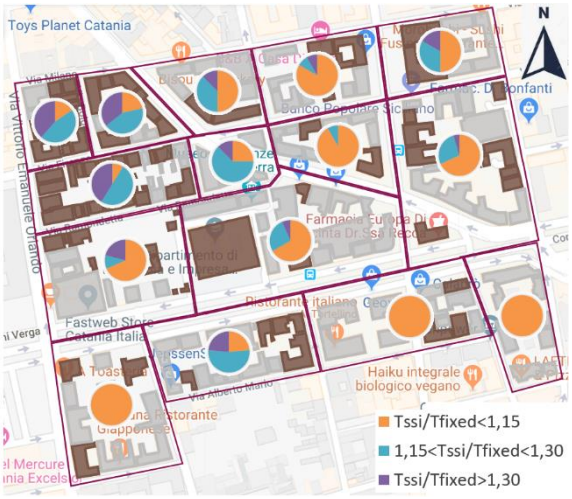

Figure 10. Spatial distribution of T_{ssi}/T_{fixed} ratios for the investigated area.

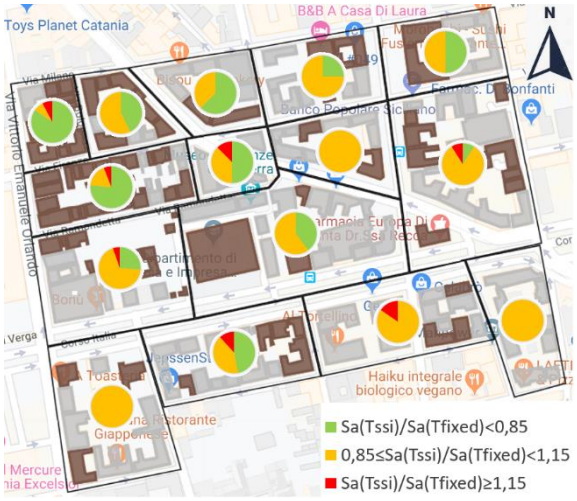

Figure 11. Spatial distribution of $S_a(T_{ssi})/S_a(T_{fixed})$ ratios for the 1693 seismic input.

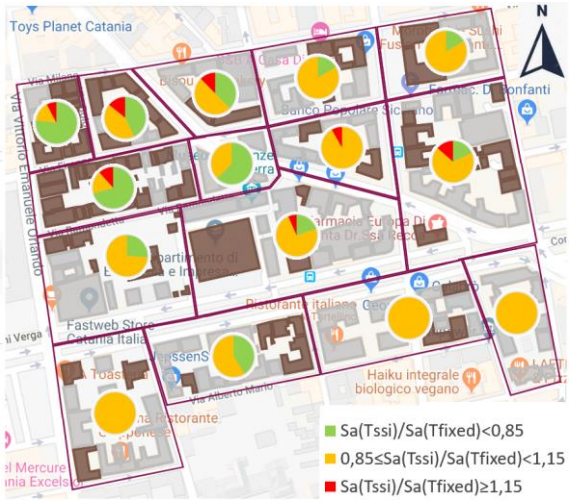

Figure 12. Spatial distribution of $S_a(T_{ssi})/S_a(T_{fixed})$ ratios for the 1818 seismic input.

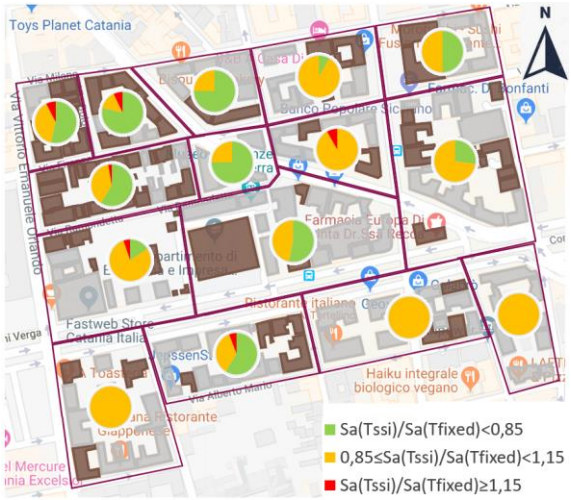

Figure 13. Spatial distribution of $S_a(T_{ssi})/S_a(T_{fixed})$ ratios for the 1990 seismic input.

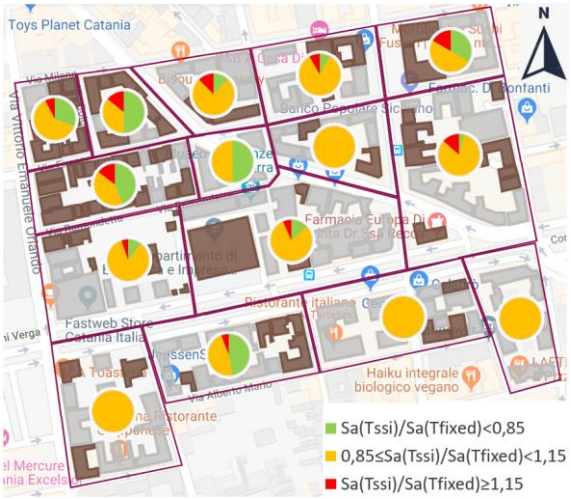

Figure 14. Spatial distribution of $S_a(T_{ssi})/S_a(T_{fixed})$ ratios for the 2002 seismic input.

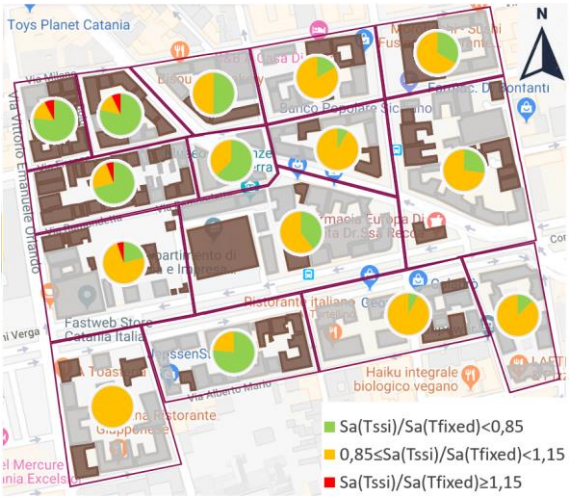

Figure 15. Spatial distribution of $S_a(T_{ssi})/S_a(T_{fixed})$ ratios for the 2018 seismic input.

Non-negligible DSSI phenomena concern mainly the "T1" stratigraphy, being constituted by poor soil.

The results show that the higher spectral accelerations ratios ($S_a(T_{ssi})/S_a(T_{fixed})$ > 1.15) are obtained for the seismic inputs of 1818 and 2002, especially in the northern part of the investigated area, i.e. for the T1 stratigraphy.

This is due both to the irregular development of the response spectra and to the nature of the foundation soil. For the rock foundation soil, i.e. for the T2 and T3 stratigraphies in the southern part of the investigated area, the spectral accelerations ratio $S_a(T_{ssi})/S_a(T_{fixed})$ are generally beneficial or negligible.

The most worrying cases are related to block "A" (34 structures). In particular, 4 structures for 1818 seismic input and 5 structures for 2002 present the higher spectral accelerations ratios ($S_a(T_{ssi})/S_a(T_{fixed})$ > 1.15); these are mainly masonry structures.

The spectral accelerations $S_a(T_{ssi})$ are finally compared with those suggested by the Italian Technical Code (NTC_2018). The results in terms of the spectral accelerations ratio $S_a(T_{ssi})/S_a(NTC18)$ are shown in Figure 16-20.

They indicate that, sometimes, just the design suggested by NTC_2018 is not always advantageous; i.e. sometimes the spectral accelerations of the flexible-base structure $S_a(T_{ssi})$ are higher than those suggested by NTC_2018 ($S_a(NTC18)$). In fact, the results show that the higher spectral accelerations ratios ($S_a(T_{ssi})/S_a(NTC18)$ > 1.15) are obtained for the seismic motions of 1693 and 2018, especially in the northern part of the investigated area, i.e. for the T1 stratigraphy.

Finally, particular interest has to be devoted to the blocks "B" (19 structures) and "F" (22 structures). They are situated on two types of foundation soil ("T1" and "T2" for the block B, "T1" and "T3" for the block F).

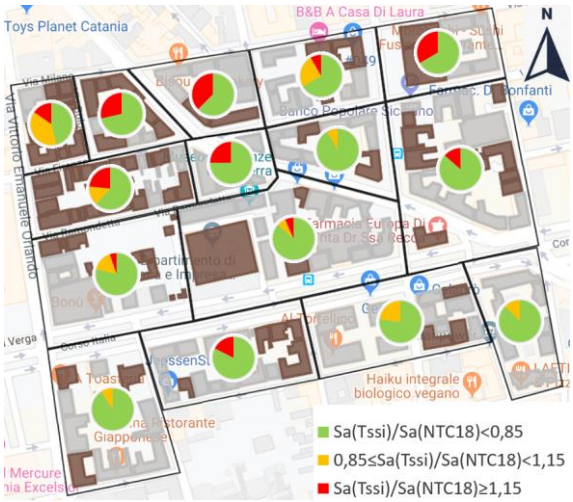

Figure 16. Spatial distribution of $S_a(T_{ssi})/S_a(NTC18)$ ratios for the 1693 seismic input.

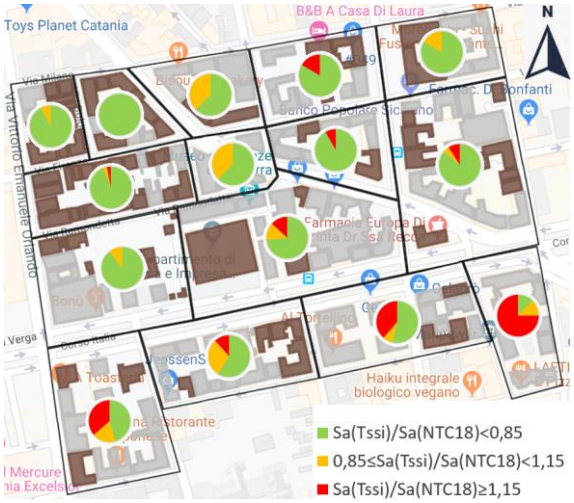

Figure 17. Spatial distribution of $S_a(T_{ssi})/S_a(NTC18)$ ratios for the 1818 seismic input.

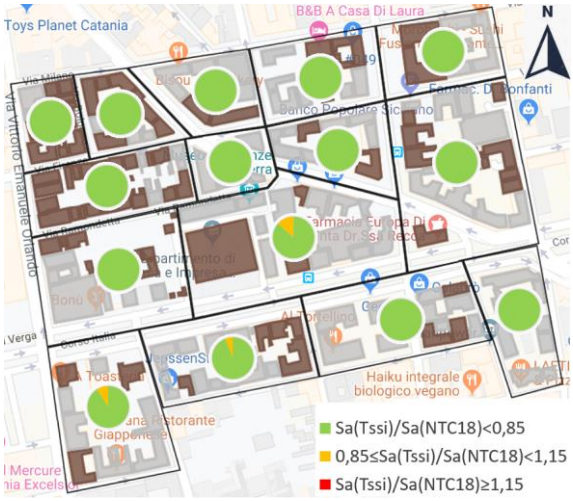

Figure 18. Spatial distribution of $S_a(T_{ssi})/S_a(NTC18)$ ratios for the 1990 seismic input.

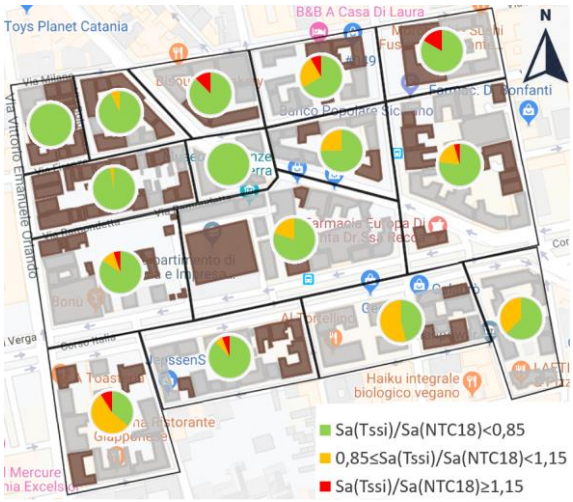

Figure 19. Spatial distribution of $S_a(T_{ssi})/S_a(NTC18)$ ratios for the 2002 seismic input.

Although, the 21% of structures situated in block "B" have high ratios of T_{ssi}/T_{fixed}, just one structure, subjected to the 1818, 2002 and 2018 seismic inputs, is characterized by high sprectral

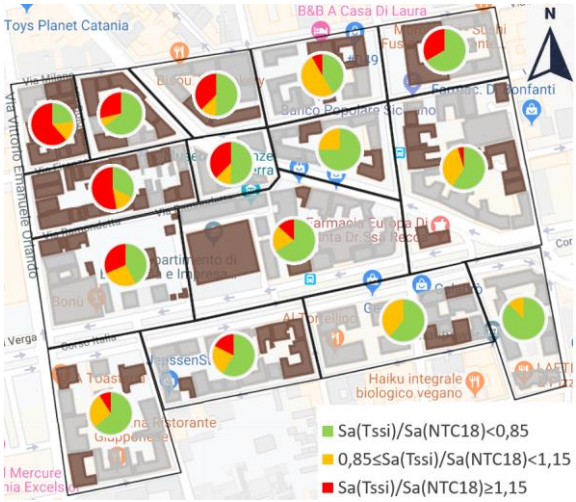

Figure 20. Spatial distribution of $S_a(T_{ssi})/S_a(NTC18)$ ratios for the 2018 seismic input.

accelerations ratios ($S_a(T_{ssi})/S_a(T_{fixed}) > 1.15$).

On the contrary, the block "F" presents only one structure having high ratios of T_{ssi}/T_{fixed}, but the 14% of structures subjected to the 1818 and 2002 seismic inputs presents high spectral accelerations ratios.

On this regard, it is very important to consider the nature of seismic input in addition to the structure's dynamic characteristics and geotechnical characteristics of the foundation soil, as well as of the whole soil-structure system. In fact, the results may be highly different with varying of the frequency and of the response spectrum of the input. In particular, it is important to compare the fundamental frequencies of inputs (shown in Table 2) with those of soils (i.e. 2.8 Hz, 3.7 Hz, 4.0 Hz for T1, T2 and T3 foundation soil respectively) and structures to understand the differences that occur when input changes.

In fact, although the fundamental frequencies of the inputs are only in a few cases close to those of the foundation soils, an important role is assumed by the frequencies of each structure which conducts different spectral accelerations ratios ($S_a(T_{ssi})/S_a(T_{fixed})$).

The results confirm once more the necessity to evaluate DSSI effects for appropriately developing subsequent seismic retrofitting of existing structures (Abate et al., 2016b), as well as seismic design of new ones (Abate et al., 2016a; 2017).

6 CONCLUSIVE REMARKS

The present paper deals with an innovative seismic microzonation taking into account DSSI effects for an area of the city of Catania.

The study shows that the DSSI effects are negligible for the majority of structures included in the examined area. So, for recent structures it would be better to consider the DSSI in order to reduce the costs of construction. However, the DSSI effects lead to adverse effects for a significant number of buildings, especially for masonry buildings. In particular, the investigated area present higher spectral accelerations ratios for the 9% and the 10% of the structures subjected to the 1818 and 2002 seismic inputs, respectively. The majority of these structures are located in soil with poor dynamic characteristics.

New areas of the city of Catania are at the moment under investigations with the same procedure shown in the present paper, for the protection and conservation of the building heritage present in Catania.

ACKNOWLEDGMENTS

Financial supports provided by the Research Project ARS01_00926 “eWAS: Un sistema di allerta precoce per il patrimonio culturale”, CUP: E66C1800039005, allowed the authors to achieve the results reported in this paper.

REFERENCES

Abate, G., Bosco, M., Massimino, M.R., Maugeri, M. (2006). Limitat state analysis for the catania fire-station (Italy). 8th US National Conference on Earthquake Engineering 2006. Volume 11, 2006, Pages 6532-6541.

Abate, G., Massimino, M.R. (2016a). Dynamic soil-structure interaction analysis by experimental and numerical modelling. Rivista Italiana di Geotecnica, 50(2), pp. 44-70.

Abate, G., Massimino, M.R., Romano, S. (2016). Finite Element Analysis of DSSI Effects for a Building of Strategic Importance in Catania (Italy). Procedia Engineering, 158, pp. 374-379.

Abate, G., Gatto, M., Massimino, M.R., Pitilakis, D. (2017). Large scale soil-foundation-structure model in Greece: Dynamic tests vs FEM simulation. COMPDYN 2017 - Proceedings of the 6th International Conference on Computational Methods in Structural Dynamics and Earthquake Engineering, 1, pp. 1347-1359.

BSSC (Building Seismic Safety Council) (2004). *National Earthquake Hazard Reduction Program (NEHRP): Recommended Provisions (and Commentary) for Seismic Regulations for New Buildings and Other Structures*. Washington DC: BSSC, FEMA 450-1 and 450–2.

BSSC (Building Seismic Safety Council) (2009) FEMA P-750—NHRP recommended seismic provisions for new buildings and other structures. Federal Emergency Management Agency, Washington, DC

BSSC (Building Seismic Safety Council) (2010). *National Earthquake Hazard Reduction Program (NEHRP): Recommended Provisions for Seismic Regulations for Buildings and Other Structures*. Washington DC: BSSC, FEMA 750.

Chopra K. A. (1995). Dynamics of Structures. Theory and Applications to Earthquake Engineering. Prentice Hall International, 1995.

Decreto Ministeriale del 14/01/2008. Norme Tecniche per le Costruzioni.

Decreto Ministeriale del 17/01/2018. Norme Tecniche per le Costruzioni.

Eurocodice 8 (2005). Progettazione delle strutture per la resistenza sismica. Parte 5: Fondazioni, strutture di contenimento ed aspetti geotecnici.

Faccioli E., Pessina V. (2000). The Catania Project: earthquake damage scenarios for high risk area in the Mediterranean. CNR-Gruppo Nazionale per la Difesa dai Terremoti - Roma.

FEMA 440 (2005). Improvement of Nonlinear Static Seismic Analysis Procedures.

Grasso S. and Maugeri M. (2005): “Vulnerability of physical environment of the city of Catania using GIS technique”. Chapter IX in: Seismic Prevention of Damage: A Case Study in a Mediterranean City. M. Maugeri Editor. WIT Press, Southampton (UK), pp. 155-175.

Grasso S., Laurenzano G., Maugeri M. and Priolo E. (2005): “Seismic response in Catania by different methodologies”. Chapter IV in: Seismic Prevention of Damage: A Case Study in a Mediterranean City. M. Maugeri Editor. WIT Press, Southampton (UK), pp. 63-79.

Gueguen P., Brad P. (2002). Site-City Seismic Interaction in Mexico City-Like Environments: An Analytical Study. Bulletin of the Seismological Society of America · March 2002

Isbiliroglu Y., Taborda R., Bielak J. (2015). Coupled soil-structure interaction effects of building clusters during earthquakes. Earthq Spectra 31(1):463–500.

Knappett J.A., Madden P., Caucis K. (2015). Seismic structure-soil-structure interaction between pairs of adjacent building structures. Geotechnique 65(5):429–441.

Kottke A. R., Rathie Ellen M., Wang X. (2013). Technical Manual for Strata. Geotechnical Engineering Center Department of Civil, Architectural, and Environmental Engineering University of Texas.

Laurenzano G., Priolo E., Klinc P., Vuan A. (2004). Near fault earthquake scenarios for the February 20, 1818 M=6.2 “Catanese” event. Proc. of the Fourth International Conference on Computer Simulation in Risk Analysis and Hazard Mitigation: “Risk Analysis 2004”, Rhodes, September 27-29, 2004; 81-91.

Massimino, M.R., Abate, G., Corsico, S., Louarn, R. (2019). Comparison Between Two Approaches for Non-linear FEM Modelling of the Seismic Behaviour of a Coupled Soil–Structure System. Geotechnical and Geological Engineering, 37(3), pp. 1957-1975.

Maugeri M. (2005). Seismic prevention of damage : a case study in a Mediterranean city. Advances in earthquake engineering, v. 14. Southampton, U.K. Boston, Mass. : WIT Press.

Rovithis E., Kirtas E., Bliziotis D., Maltezos E., Pitilakis D., Makra K., Savvaidis A., Karakostas C., Lekidis V. (2017). A LiDAR-aided urban-scale assessment of soil-structure interaction effects: the case of Kalochori residential area (N. Greece). Springer Science + Business Media Dordrecht 2017.

Veletsos A.S., Meek J. (1974). Dynamic behavior of building-foundation systems. Earthq Eng Struct Dyn 3:121–138.

Veletsos A.S., Verbic B. (1973). “Vibration of Viscoelastic Foundations”. *Earthquake Engineering and Structural Dynamics*, 2(1):87-105.

Worku A. (2014). Soil-structure-interaction provisions. A potential tool to consider for economical seismic design of buildings? Journal of the South african inStitution of civil engineering.